Wave Spectra Derived by CWT on the Radar Images

Dong Jiing Doong[1] Lee Chung Wu[2] Chia Chuen Kao[3] Laurence Zsu Hsin Chuang[4]

Coastal Ocean Monitoring Center,
National Cheng Kung University,
No.1, Da-Shue Rd., Tainan, Taiwan 701, Republic of China
[1]doongdj@yahoo.com.tw [2]n8689405@ccmail.ncku.edu.tw [3]kaoshih@mail.ncku.edu.tw
[4]laurence@mail.ncku.edu.tw

Abstract

Ocean waves, which feature extremely random, affected by the meteorological factors, atmospheric factors, topological conditions and currents. Wave spectra are the fundamental presentation of ocean waves, which express the energy distribution as a function of component waves. It is an advantageous tool on investigating the processes of the wave generation, propagation, and can be used in the applications of wave forecasting and coastal engineering. In addition to the in-situ measurements, excelling at wide range of spatial coverage, remote sensing should be the trend in the future wave field measurement.

There are some deficiencies found in the previous study of analysis the wave field using satellite images. One of the most important reasons is that the satellite is not suitable to apply to the nearshore area where is a high non-homogeneous water. The potential land-based marine radar image is test in this study. In order to analysis the nonhomogeneous images, the continuous wavelet transform (CWT) was adopted. In this study, the CWT algorithm on wave spectra analysis was derived and developed. Several simulation images and the real radar image were analysed. This study show that the wavelet transform has excellent performance to the wave components detection. However, more research on the real radar images is needed to intensify the results.

1 Introduction

Wave, among other natural phenomena, is the most complex and predominate factor to coastal and ocean engineering, considering the functional and structural design. It cannot be fully understood only by numerical or physical models. Field data measurement and analysis must also be performed to increase the knowledge of waves. The directional spectra are the fundamental presentation of ocean waves, which express the energy distribution as a function of wave frequency and wave propagation direction. The frequent approaches for the directional wave measurement could be categorized as In-Situ measurement and Remote Sensing Techniques. Regarding the In-Situ measurement, the data buoy and pile station equipped with wave gauge array have been developed since mid 60's. After years of improvement and calibrations, currently they are widely implemented as routine operational oceanographic monitoring systems. The results are offered as reference of oceanographic forecasting and engineering applications. On the other hand, the remote sensing technology is a new approach, which provides extensive sets of ocean surface data. It features good capability at wide range of spatial coverage.

There is severe sea state in Taiwan due to the monsoon waves in the winter season, and typhoon induced waves and storm surge in the summer season as well. However, most coast engineering and human activities take place in nearshore areas. In response to obtain the high quality meteorological and oceanographic data for engineering design or safety construction, an monitoring network comprising Data Buoys and other automatic observation systems is planned and is being set-up in Taiwan by Coastal Ocean Monitoring Center (COMC) of National Cheng Kung University. Real-time field data from these operational observation systems have been used for weather forecasting and warning, model validation, engineering design and others requiring accurate measurements and reliable performance. Besides the in-situ observations, the COMC is also attempting to collect data over broader areas using remote sensing techniques. This effort seeks to extend the coastal ocean information from point to spatial observations.

The radar images of the Earth's surface represent the spatial pattern of reflected microwave energy. Imaging radar as shown in Table 1 is one of the active microwave sensors and is classified into Real Aperture Radar (RAR) and Synthetic Aperture Radar (SAR). The RAR means a radar whose signal beamwidth is controlled by the physical length of the antenna. The SAR means a radar whose antenna length is synthesized using sophisticated processing techniques. RAR receives its backscatter from the same location as the initial transmitted microwave signal. However, SAR sends out a signal, but uses the forward motion of the moving platform to receive the backscatter over a distance, thus simulating a larger aperture. This simulated aperture and the more sophisticated signal processors allow for higher resolution than a standard aperture sensor. Typical spatial resolution of image radar is 10 to 30 meters. This resolution is similar to some high resolution visible/IR

sensors, but SAR/RAR sensors can collect data independent of weather or light conditions.

Table 1 Functions of active microwave sensors [excerpt from JARS, 1999][5]

Sensor		Functions (Target)
Active sensor	Microwave scatterometer	-Soil moisture -Surface roughness -Distribution of ice / snow -Sea state, sea surface wind and temperature -Precipitation intensity
	Microwave altimeter	-Sea surface topography -Ocean wave height -Meso-scale eddy, tide -Wind velocity
	Imaging radar (SAR/RAR)	-Image of surface ocean wave -Near sea surface wind -Submarine topography -Monitoring of ice

In coastal oceanography, SARs have demonstrated their ability to record internal waves, surface waves, bathymetric features, and the location of ocean fronts (Forget and Brosche, 1996). In the open ocean, the frontal location of major currents can be observed and measured (Liu et al., 1994). Also, SAR images are also useful to detect the marine pollution. SAR imaging of surface gravity waves in the ocean has been demonstrated by many investigators, although the relative importance of imaging mechanisms such as hydrodynamic of modulation, tilt modulation, and velocity bunching is still not that well understood (Hasselmann et al., 1985 and Alper et al., 1986). However, there are still many studies for examing the evolution of wave fields, and the wave-current interactions using SAR images (Peng et al., 1995; Beal et al., 1986). By the continuous studies, scientists may well improve their knowledge of the circulation and dynamics of global oceans from these techniques and from data being collected by the SAR systems.

Nonetheless, consider the return time and the maintain costs, the satellite SAR is not so suitable on the operational purposes. In addition, some limitations and the non-performable results of the spectra analysis on the nearshore images were found in the authors' previous study [7]. Therefore, the potential marine radar image is planning to be adopted for the future study of waves. The marine radar wave monitoring device belongs to the RAR system. It is a land-based system; therefore it is of comparatively ease of setup and maintenance. The risk of lost or damaged in the severe sea climate can be reduced. There was a wave monitoring system (named WaMoS) developed at the GKSS research center in Germany (Ziemer, 1991; Dittmer, 1995) [2][10]. Although the marine radar system is capable to operate routinely, it still needs more validity check and calibration.

The paper is organized as follows: in section 2, the transform method to derive the image spectra is derived. The SAR spectra are calculated and the limitations of SAR devices are discussed in section 3. In section 4, results of RAR spectra derived by CWT on simulation and true images are outcome. The summary and conclusions are given in section 5.

2 Transform the radar backscatter to image spectra

2.1 The Fourier transform

Satellite images record the two-dimensional distribution of back scattering strength of satellite radar echoes of the sea surface. A two-dimensional fast Fourier transform (2D FFT) is directly used to convert these signals into wave spectra information. The discrete values of $g(\vec{x})$ corresponding to the level of gray of each pixel. The Fourier transform is defined, as usual, by

$$\hat{s}(\vec{k}) = (2\pi)^{-1} \int e^{-i\vec{k}\cdot\vec{x}} g(x,y)dxdy \qquad (1)$$

In this equation, $\vec{k}$ is the wavenumber vector. The square of Fourier coefficients can be used to derive the image wavenumber spectrum, which in turn allows the wave energy and wavelength distribution in the x-y perpendicular coordinate plane to be obtained. Due to the directional spectrum is the spectral energy expressed in terms of directional and frequency distribution. It is therefore necessary change the two-dimensional perpendicular coordinate wavenumber spectrum into a polar coordinate wavenumber spectrum. The idea to convert wavenumber spectra into directional wave spectra using a dispersion relationship equation which used by Kuo et al. (1999) [6] was adopted in this study.

2.2 The Continuous Wavelet Transform (CWT)

The two-dimensional Fourier transform uses a single window encompassing the entire image. Thus, information about surface patch non-periodic variations with distance is not readily available from the spectrum. The continuous wavelet transform (CWT) uses small windows at high frequencies (or wavenumber) and large windows at low frequencies. The result is a distance-frequency decomposition of the image into wavelet coefficients. The frequency resolution decreases with increasing frequency to produce constant relative frequency resolution. The distance resolution increases with increasing frequency to aid in identifying wave structure visibility is reduced or masked by surface patch variations can be identified by variable wavelet coefficients. Given a 2D image signal s, its CWT with respect to the analyzing wavelet ψ is as following.

$$F(\vec{a},\vec{b}) = \int_{-\infty}^{\infty}\int_{-\infty}^{\infty} G(x,y)\cdot\psi_{\vec{a},\vec{b}}(x,y)dxdy \qquad (2)$$

where the $\vec{a}$ is the scale parameter and $\vec{b}$ is the shift parameter. A wavelet is an admissible signal, that is, a complex-valued function, which satisfies the admissibility condition

$$C_\psi \equiv (2\pi)^2 \int d^2\vec{k}\left|\vec{k}\right|^{-2}\left|\hat{\psi}(\vec{k})\right|^2 < \infty \qquad (3)$$

where $\left|\vec{k}\right|^2 = \vec{k}\cdot\vec{k}$ if ψ is regular enough. The admissibility condition simply means that the wavelet has zero mean:

$$\int\psi(\vec{x})d^2\vec{x} = 0 \qquad (4)$$

2-2.1 Choose of the wavelet function

The wave transform analysis result depends on the choice of a fixed analyzing wavelet. The choose of the wavelet function depends on the goal one pursues. The only practical requirements are that ψ be fairly well localized in the space domain ($\vec{x}$) and in the spatial frequency domain ($\vec{k}$). There are powerful theorems that guarantee the existence of a wavelet that generates a family with special properties. But, in 2D case, such wavelets are only available in Cartesian geometry, and such theorems are of little help in practice. In addition, due to the inherent orientation characteristic, the Morlet wavelet is good at detecting directional features and is choused in this study. Its general form is the following:

$$\psi(\vec{x}) = e^{i\vec{k}_0\vec{x}}e^{-\frac{1}{2}(\vec{x}\cdot A\vec{x})} - e^{-\frac{1}{2}(\vec{k}_0\cdot B\vec{k}_0)}e^{-\frac{1}{2}(\vec{x}\cdot A\vec{x})} \qquad (5)$$

The second term in (5) is a correction that guarantees that ψ satisfies the admissibility condition $\hat{\psi}(0) = 0$. If $\left|\vec{k}_0\right|$ is chosen large enough, typically $\left|\vec{k}_0\right| \geq 5.5$, this correction term is numerically negligible.

2.2.2 The relationship between ($\vec{a},\vec{b}$) and ($\vec{x},\vec{k}$)

On the 1D signal, the coefficients of wavelet transform relates to the time and frequency parameters in the spectra. However, the wavelet coefficients ($\vec{a},\vec{b}$) have the relationship with position and the wavenumber ($\vec{x},\vec{k}$). The wavenumber distribution of an image pattern is calculated from the scale parameters of wavelet transform. The formulation is derived in this study as following.

$$k_x = \frac{k_x^*}{a_x} = \frac{\sum_0^\infty k_x \times \left|\exp\{[-0.5\times(k_x^2 + (k_y - k_{y0})^2)]\}\right|^2 \Delta k_x}{a_x\sum_0^\infty \left|\exp\{[-0.5\times(k_x^2 + (k_y - k_{y0})^2)]\}\right|^2 \Delta k_x} \qquad (6)$$

The relationship between k_y and a_y can be derived in the same way. On the other hand, the position of the component wave (k_x,k_y) was also derived from the wavelet coefficients. The formulation of position x is outlined as following. The position y can also derived the formulation of the relationship between shift parameter and the position in the image was also be derived.

$$x = b_x + a_x \cdot \frac{\sum_0^\infty t_x \left| e^{-2i(\omega_{0x},\omega_{0y})\cdot(x,y)}\cdot e^{-\frac{1}{2}|\vec{x}|^2}\right|^2 \Delta x}{\sum_0^\infty \left| e^{-2i(\omega_{0x},\omega_{0y})\cdot(x,y)}\times e^{-\frac{1}{2}|\vec{x}|^2}\right|^2 \Delta x} \qquad (7)$$

3 Wave Spectra on ERS-1 SAR image

3.1 SAR Wave Fields in the offshore and nearshore coast

In this section, the image spectra of SAR image from the spacecrafts that launched by European Remote Sensing Satellites (ERS-1/2) were brief reported [7]. The SAR image on Feb. 7, 2000 is shown in Fig. 1. The 128 × 128 pixels subimage was suggested to be used in the SAR images analysis in the previous study [7]. The frames in the photo delineate the nearshore and offshore subimages used in the following studies.

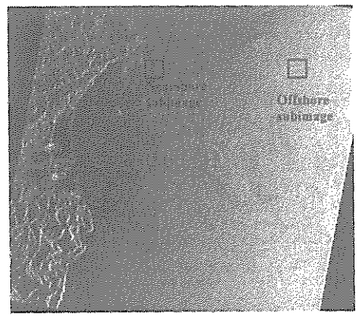

Fig. 1. SAR image of the Northeastern Taiwan Waters

Fig 2 is the wavenumber spectra of performable offshore subimage, however the non-performable spectrum of the nearshore subimage is shown in fig. 3. A comparative study of 11 SAR images with in-situ measurements are done. The results were shown that not every SAR images could be used to perform wave field analysis. The average wavelength discrepancy of the comparison on the nearshore images was approximately 16%, while the averaging wave direction discrepancy was approximately 12°. The discrepancy is larger in nearshore image than those in deep water.

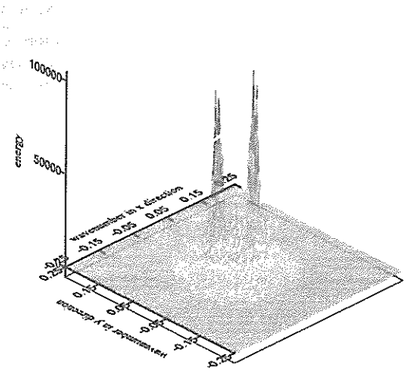

Fig. 2. The wavenumber spectra of performable subimage in the offshore water

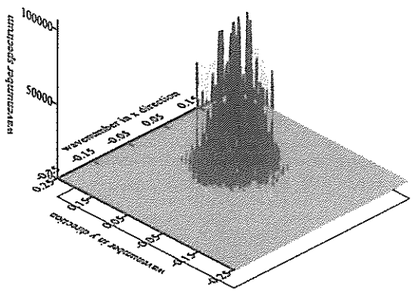

Fig. 3. The wavenumber spectra of non-performable subimage in the nearshore area

3.2 Some deficiencies on the use of SAR to analyse ocean waves

The issues on the effect of (1) relationship between satellite travel and wave propagation direction and (2) the distribution of image gray values were discussed for the limitation of SAR spectra analysis in previous study. The results show that the closer the flight direction of satellite to the wave prorogation direction, the greater error between SAR and in-situ measurement. The higher the average value of an image's gray value, the harder it is to distinguish the wave direction and wavelength from image analysis.

Besides, the wavelength of ocean wave will vary as it moves from deeper water into the nearshore area as the wave direction may also change due to the effects of reflection and refraction. It shows that the spatial wave field in nearshore waters is unlikely to be uniform. If a nearshore SAR image contains large variations in water depth, the spatial wave field distribution in the image will tend be extremely nonhomogeneous. It's not appropriate to use a "characteristic" wave parameter to describe the complex spatial wave field in the nearshore waters. It's one of the reasons on the result of Fig. 3.

4 Wave Spectra on Marine Radar (RAR) image

Due to the deficiencies of the SAR applications, the commercial marine radar was considered to measure the ocean features. The marine radars have been used to measure the directional distribution of the sea surface elevation for several years. The sea clutter is considered as noise for navigation purposes. However, these data can be analyzed to determine sea state parameters, such as wave spectra, wave periods, propagation directions, significant wave eights, etc [2][10].

4.1 Spatial wave fields Simulations

In order to test the performances of the wavelet transform that be applied to the nonhomogeneous spatial wave field. The image that contains four component patterns was simulated. The parameters of the nonhomogeneous image simulation are shown in Table 2.

Table 2 The parameters of the image simulation

	A_i	L_i	θ_i
Component wave 1	15	15	$\pi/4$
Component wave 2	15	5	$\pi/3$
Component wave 3	15	5	$-\pi/6$
Component wave 4	15	10	$\pi/2$

Fig. 4 is the simulated image. There are four patterns that locate in the four quadrants respectively. The wavenumber spectrum by using the Fourier transform is shown in Fig. 5. There were four visible components of the image found in the spectra domain. They happen in the positions (0.31,0.31), (1.0,0.70), (-0.61,0.83) and (0,0.63) of the (k_x,k_y) wavenumber domain, the corresponding component lengths and directions exactly equate to the input parameters. However, the Fourier representation is an average outcome, which can't show the homogeneous characteristics in the image.

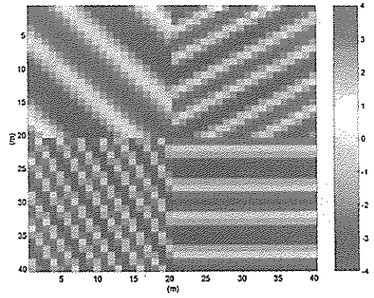

Fig. 4. The 2D simulated wave image

(4 component waves)

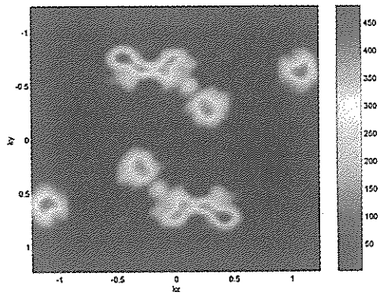

Fig. 5. The Fourier Spectrum of the simulated image

4.2 The wavenumber representation: (k_x,k_y) fixed

It's uneasy to show the analysis outcome of wavelet transform because of that there are four variables after the transform: two position variables, two frequency variables. This fact explains the efficiency of the CWT in treating singularities, since it unfolds them from two to four dimensions, but it also creates difficulties, both at the computational level and for the visualization of the results. These problems are solved by restriction to suitable 2D sections of the 4D parameter space and systematic recourse to the FFT algorithm.

The first natural possibility is to consider the transform as a position function of (x,y) alone, for the wavenumber (k_x,k_y) fixed. This representation is useful for general purposes of image analysis, such as detection of position, shape and contours of objects, form recognition. Fig. 6 shows the wavelet spectrum of the simulated image that (k_x,k_y) was fixed at (0,0.628) and Fig. 7 is the wavelet spectrum at (k_x,k_y) =(0.31,0.31). The spectra identify the features of components of No.1 and No.4.

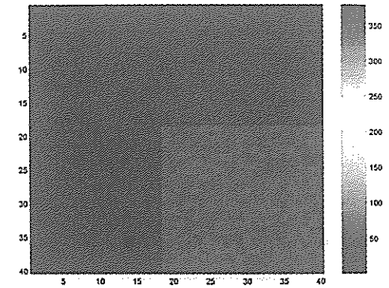

Fig. 6. The wavelet spectrum of the simulated image

$[(k_x,k_y)=(0,0.628)]$

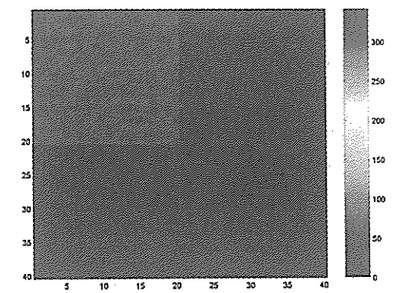

Fig. 7. The wavelet spectrum of the simulated image

$[(k_x,k_y)=(0.31,0.31)]$

4.3 The position representation: (x,y) fixed

The opposite possibility consists in fixing (k_x,k_y) and considering the CWT as a function of (x,y). In the other words, the CWT is looked at one position and examined at all scales and in all directions. This position representation is useful for several applications, such as fractal recognition or the determination of local wave. Fig. 8 and Fig. 9 are the wavelet spectra of the simulated image that fixed the point at (5,5) and (30,30). The spectra show only one single component in the figures that equals to the default pattern in Fig. 4.

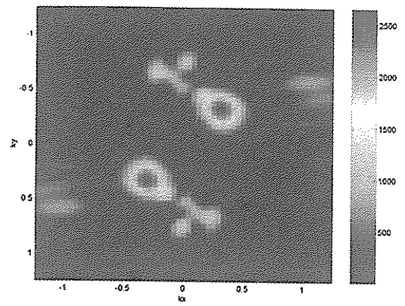

Fig. 8. The wavelet spectrum of the simulated image

$$[(x, y) = (2,2)]$$

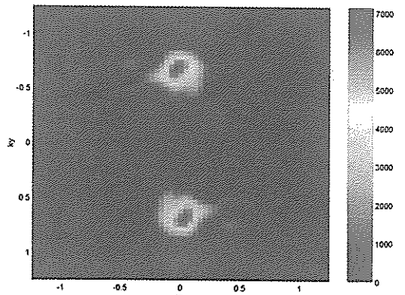

Fig. 9. The wavelet spectrum of the simulated image

$$[(x, y) = (38,38)]$$

4.4 Field Radar image analyses

By the simulation studies, we identify the performance of wavelet transform. The function of the detection on component positions is better than Fourier algorithm. In this section, the real radar image is going to be analyzed. One wave scanning system based on the X-band marine radar was developed in the Institute of Oceanography of National Taiwan University. The system is composed by commercially marine radar and an A/D converter plus a program to analyze the sea clutter.

The wave scanning system is setup in the Mailiao harbor in the western Taiwan. Mailiao harbor is located at longitude 120°08.9' E, latitude 23°46.9' N. The shipping channel is 24 meters deep at mean tide, making it Taiwan's deepest harbor and the first harbor constructed and operated by a private company. The harbor entrance faces to west with inclination 34 degrees to south direction. The west breakwater is 3243 meters long, and the south breakwater is 2227 meters long as show the radar image in Fig. 10.

To analyze the data a quadrate region with the size of 128×128 pixels (1.92 km × 1.92 km) was cut out of the full radar image as show in Fig. 11. Fig. 12 is the position representation at point (50,50) of the radar subimage.

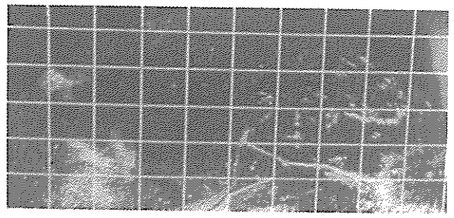

Fig. 10. The full marine radar image in Mailiao Harbor

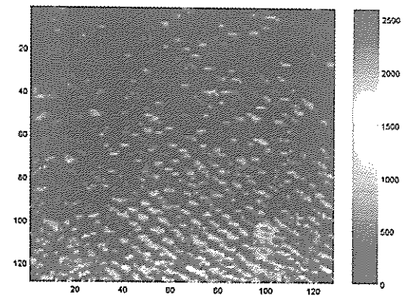

Fig. 11. The 128×128 pixels marine radar sub-image

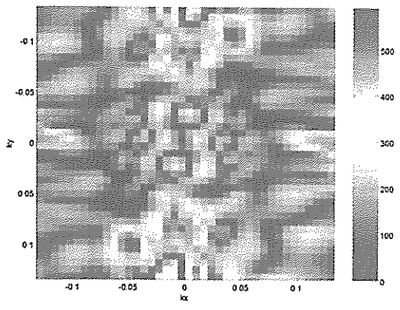

Fig. 12 The wavelet spectrum of the radar subimage at $(x, y) = (50,50)$

5 Summary and Conclusions

Oceanographic information from remote sensing instruments provides an extensive set of ocean surface data. The remote image is a 2D sampling of the back scattering strength of echoes of the sea surface over a specific area. For many years, the satellite SARs are nearly the only sensor capable of obtaining global samples of ocean spectra from space. However, this study found that:

1. Not every SAR images can be used to analysis the wave spectra.

2. The comparative studies show that the difference of significant wave parameters between nearshore SAR derivation and in-situ measurements was larger than those in deep waters.

Besides, due to the highly non-homogeneous wave field in the nearshore area, the SAR is difficult to analysis the wave spectra with FFT algorithm. Consider the operational function and the costs of maintenance, the land-based marine radar is used to the nearshore wave measurements.

In order to analysis non-homogeneous wave field, the powerful CWT algorithm was preliminary developed in this study. First test was on the simulated 2D wave images and then applied to the true radar image. The results show that the component waves can be located correctly by wavelet transform in the wavenumber fixed representation. By this function, the wavelet transform can be applied to discuss the distribution of any interested component waves in the full radar image. Furthermore, the evolution of located component waves on time domain is also achievable by applying the wavelet transform to 3D radar images.

6 Acknowledgments

This study was financial support by the National Science Council, R.O.C. (NSC 89-2611-E006-074). A special thanks is given to Prof. Joe Wang in the Institute of Oceanography of National Taiwan University for providing the marine radar images data used.

7 References

[1]Alper, W. R. and Bruening, C. (1986), "On the relative importance of motionrelated contributions to the SAR imaging mechanism of ocean surface waves", IEEE Transactions on Geosciences and Remote Sensing, GE-24, pp. 873-885.

[2]Beal, R. C., Gerling, T. W., Irvine, D. E., Monaldo, F. M. and Tilley, D. G. (1986), "Spatial variations of ocean wave directional spectra", Journal of Geophysics Research, 91(C2), pp. 2433-2449.

[3]Chuang, L.Z.H., Kao, C.C. and Lee, B.C. (1998), "The Development of Operational Data Buoy System in Taiwan", International Conference on Marine Disaster: Forecast and Reduction, Beijing, China, pp.101-110.

[4]Dittmer, J. (1995), "Use of marine Radars for Real Time Wave Field Survey and Speeding up the Transmission/Processing". Proceeding of the WMO/IOC Workshop on Operational Ocean Monitoring using Surface Based Radars, Geneva.

[5]Forget, P. and Broche P. (1996), "Slicks, Waves, and Fronts Observed in a Sea Coastal Area by an X-band Airborne Synthetic Aperture Radar" Remote Sensing Environ. 57(1), pp.1-12.

[6]Hasselmann, K., Raney, R. K., Plant, W.J., Alpers, W., Shuchman, R.A., Lyzenga, D.R., Rufenach, C.L. and Tucker, M. J. (1985), "Theory of synthetic aperture radar ocean imaging: A MARSEN view", Journal of Geophysics Research, 90, pp.4659-4686.

[7] Japan Association of Remote Sensing (JARS) (1999), "Remote Sensing Notes"edited by Japan Association of Remote Sensing.

[8]Kuo, Y.Y., Leu, L.G. and Kao, I. L. (1999), "Directional spectrum analysis and statistics obtained from ERS-1 SAR wave images", Ocean Engineering, Vol. 26, pp.1125-1144

[9] Lin, H. P., Doong, D.J., Chuang, L. Z. H. and Kao, C.C. (2000), "Some Notes on the Nearshore Wave Field Analysis Using SAR Images", Proceedings of the 22th Ocean Engineering Conference in Taiwan, pp.384-392, Taiwan. (in Chinese)

[10]Liu, A.K., Peng, C.Y. and Schumacher, J.D. (1994), "Wave-current interaction study in the Gulf of Alaska for detection of eddies by SAR", Journal of Geophysics Research, 99, pp.10075-10085.

[11]Peng, C.Y. and Liu, A.K. (1995), "SAR observations of interaction of ocean swell and Semidi Inlands in the Gulf of Alaska", International J. Remote Sensing, 16, pp.1249-1260.

[12]Ziemer F. (1991), "Directional Spectra from Shipboard Navigation Radar during LEWEX", Directional Ocean Wave Spectra, Edited by Robert C. Beal, The John Hopkins University Press.

Inaugural International Conference on Port and Maritime R & D and Technology
Singapore, 29 - 31 October 2001